



A medical robot for needle placement therapy in liver cancer^{*}

Xing-guang DUAN[†], Gui-bin BIAN, Hong-hua ZHAO, Xing-tao WANG, Qiang HUANG

(Intelligent Robotics Institute, Beijing Institute of Technology, Beijing 100081, China)

[†]E-mail: duanstar@bit.edu.cn

Received Jan. 19, 2010; Revision accepted Jan. 27, 2010; Crosschecked Jan. 27, 2010

Abstract: Hepatocellular carcinoma (HCC) is the second most common malignancy in China. As microwave ablation (MWA) is an effective method for liver cancer, a robotic surgical system with ultrasound-directed was designed to assist surgeons on positioning the needles. This robotic system includes a surgical robot with 5 degrees of freedom, a workstation for path-planning and image processing, a conventional 2D ultrasound device, and an electromagnetic (EM) tracking system. Surgery space, clinical operation requirements and optimal mechanical structure are the key factors to be considered in designing a medical robot suitable for use by surgeons. Based on the mechanics of the needle placement robot, we have conducted detailed kinematic analysis, including a combined numerical algorithm and coordinate mapping. Finally, the feasibility of the needle placement robot has been validated by experiment.

Key words: Surgical robot, Needle insertion, Inverse kinematics, Numerical solution

doi: 10.1631/jzus.A1000040

Document code: A

CLC number: TH6

1 Introduction

Hepatocellular carcinoma (HCC) is one of the most common malignant neoplasms in the world (Colombo, 1992), causing more than one million deaths worldwide annually (Esquivel *et al.*, 1999). In China, it is the second most common malignancy. Current treatments for HCC mainly include surgical resection and ablative treatment. Unfortunately, most patients with primary and secondary liver cancer are not suitable for resection, primarily due to tumor location or underlying liver disease.

A number of clinical studies have shown that microwave ablation (MWA) is an effective and safe treatment for liver cancer (Seki *et al.*, 1994; 1999). Current clinical MWA, however, is manually performed by surgeons. It strongly depends on the surgeon's needling skills against hand's tremor, hand-eye coordination and concentration. Now only a few

surgeons are experienced and capable enough to use MWA, which limits its wider usage.

For these above reasons, it would be advantageous to develop a robotic system to assist surgeons in MWA treatment. Boctor *et al.* (2004) proposed two robot arms for intra-operative ultrasound-guided hepatic ablative therapy. The two robot arms conduct both ultrasound manipulation and needle guidance, overcoming the problem of freehand ultrasound. The system, however, is complicated by having two manipulators, which increases the system's failure rate, and is more cumbersome in the clinic setting.

In this paper, we present a robotic system to assist surgeons on MWA treatment for HCC patients. The robot arm is under the guidance of 3D ultrasound (3DUS), reconstructed from a conventional 2DUS device by 3D freehand reconstruction. This system allows for automatic control of the robot arm, by which the surgeon inserts the needle into the tumor target. This surgical robotic system can position the needle into the liver tumor more accurately and overcome the problem of hand tremor, so that the surgeon can concentrate more on planning and monitoring the procedure.

^{*} Project supported by the National High-Tech (863) Research and Development Program of China (No. 2006AA04Z216), and the National Natural Science Foundation of China (No. 60875054)

© Zhejiang University and Springer-Verlag Berlin Heidelberg 2010

2 HCC and its treatment

HCC is a liver disease (Fig. 1), which occurs most frequently in Asia, southern Africa and the Pacific Rim area than in other parts of the world. The age range of patients with HCC is wide, but most are over 40 years old.

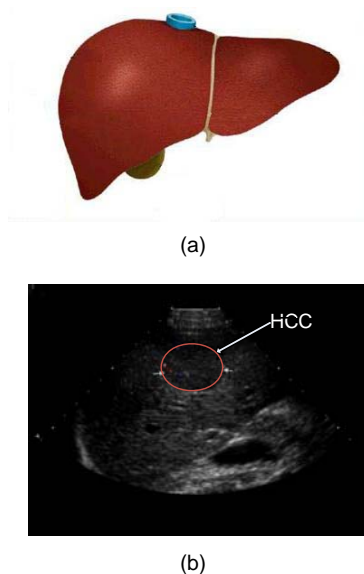


Fig. 1 Liver cancer (a) and the ultrasound image of HCC (b)

The formation of HCC is a slow process, during which genomic changes progressively alter the hepatocellular phenotype to produce cellular intermediates which evolve into HCC (Thorgeirsson *et al.*, 2002). During the long preneoplastic stage, it is difficult to detect, and because of late diagnosis, difficult to treat. Studies indicate that hepatitis B virus, hepatitis C virus, long-term use of aflatoxin and genetics are important etiologic factors. Currently, there are two major treatments for HCC, surgical treatment and non-surgical treatment (Ye and Qin, 2008).

The surgical treatment is most often applied in the following cases:

1. Patients are generally in good condition without significant heart, lung, kidney, or other serious organic disease;
2. Liver function is normal, or there is only slight damage (Child-Pugh grade A), or liver function is at grade B and after short-term treatment it can return to grade B or better;
3. The liver functional reserve is within the normal range;

4. No unremovable metastatic liver tumor is present.

Most liver cancer patients, however, are not suitable for surgical resection because of their poor liver function, the multi-center location of the tumor, and other factors.

MWA is an alternative, a non-surgical treatment characterized by greater procedural simplicity, effective tumor inactivation, and fewer complications. MWA treatment is most often applied in the following cases:

1. Single tumor and tumor ≤ 5 cm in diameter;
2. Multiple tumors, with the number of tumors ≤ 3 , the largest tumor $\leq 3-4$ cm in diameter;
3. No tumor embolus in blood vessels and gall vessels, or transfer lesion outside the liver;
4. The distance between liver tumor and liver's main vessel is at least 5 mm.

Current MWA treatments are manually performed by surgeons. The general surgical procedure is as follows. First, a computed tomography (CT) scan is taken over the zone about and around the patient's liver; from the CT image, the surgeon can position the HCC tumor and thereafter consider a needle path taking into account the surrounding anatomy including vessels and other important structures. Then, using the 2DUS-directed image, the surgeon inserts the needle along the pre-planned path to the center of liver tumor. The surgical performance, however, relies on surgeon's superior experience and judgment. Furthermore, it also depends on the surgeon's needling skills against hand tremor, hand-eye coordination and concentration. Therefore, we developed a US-directed robotic system to assist the surgeon in positioning the needles for the MWA treatment.

3 System overview

Fig. 2 describes the overall structure of a 2DUS guided robotic system for MWA in liver cancer. Major system components include:

1. A PC-based surgical workstation providing overall application control, 2DUS and 3DUS processing, surgical planning and surgeon interfaces.
2. A conventional 2DUS device (WEUT-70X ultrasound machine, China-well, Inc.), which is connected to surgical workstation via video cable.

(3) A 5-degree of freedom (DOF) needle placement robot for positioning a needle guide for MWA controlled by the workstation via RS-422.

(4) An electromagnetic (EM) tracking system (Fastrak, Polhemus, Inc.), which is connected to the surgical workstation via USB, and which is used to position the robot arm and attain 2DUS images' positions and orientations to fulfill the 3D model reconstruction.

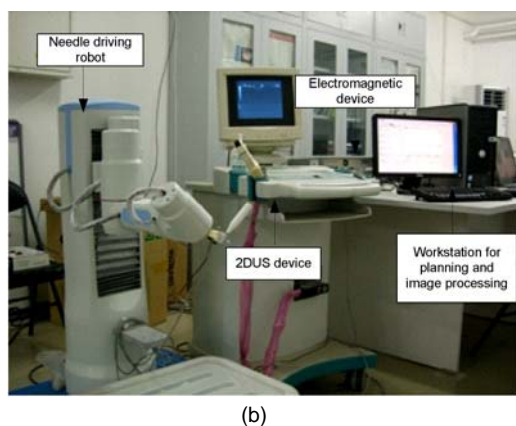
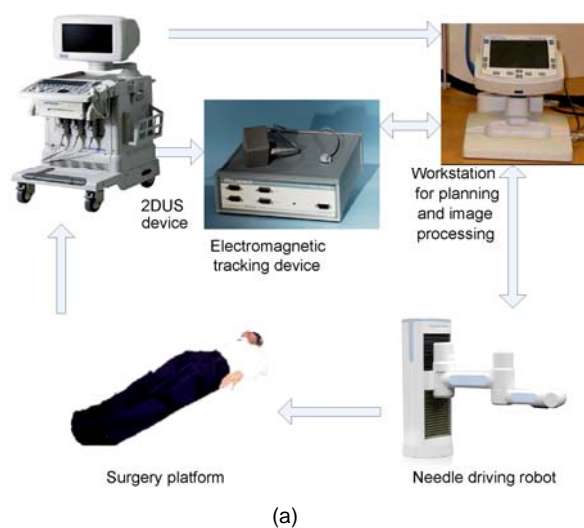


Fig. 2 Overall structure of US-directed robotic system for MWA in liver cancer. (a) System architecture; (b) Experimental setup

4 Mechanical design

Effective and rational mechanical structural design of the robot system is the foundation of the entire system (Cleary and Nguyen, 2001). Tsai and Soin (1984) synthesized a robot with two or three links

according to the design charts of the working space. They also divided the robot into two parts, the position structure and the orientation structure (Tsai and Soin, 1985). From this aspect, the impact of structural parameters and motion parameters on the position and posture could be analysed to inform the design of other robots. Ying and Ma (1991) summed up the simple specification program, using a level-screening method for mechanical design. We adopted the screw theory to design the mechanic of robot assisting MWA.

Based on the requirements of operating tasks, operating environments, and workspace area, we designed a 5-DOF robot including a robot arm with three DOFs and a robot wrist with two DOFs as shown in Fig. 4. This structure can also attain very precise positioning. The first DOF of the robot arm is vertical movement, while the other DOFs rotate in the level plane. The position of the tool in the selected working plane is determined by three DOFs. The required posture of the surgical tool within workspace is controlled with the two DOFs of the wrist. This mechanical structure has the advantages of having a small-size, large-scope, high-precision positioning and ease of use in operation. There is also the availability of kinematics analysis.

The parameters of the robot are shown in Table 1. The scope and speed of each axis are shown in Table 2.

Table 1 Parameters of the robot

Parameter	Value
DOF	5
Dimensions*	800×230×680 (when the arms expand) 550×320×680 (when the arms fold)
Weight (kg)	25
Custom speed (mm/s)	20
Drive mode	DC brush motor
Driver power	24 V DC
Control power	12 V DC

* length×width×height, mm×mm×mm

Table 2 Scope and speed of each axis

Joint	Motion scope	Maximum speed
Prismatic joint	300 mm	100 mm/s
Joint 2	55°	20 (°)/s
Joint 3	110°	20 (°)/s
Joint 4	90°	40 (°)/s
Joint 5	90°	40 (°)/s

4.1 Robot arm

The robot arm with three DOFs can reach any position within the operating space. Currently, the typical configurations of robot arm patterns are: articulated configuration, cylindrical configuration, selective compliance assembly robot arm (SCARA) configuration, Cartesian configuration and polar configuration.

Arm structures of minimally invasive surgery robots mostly utilize the cylindrical configuration (ROBODOC), SCARA configuration (ZEUS) and Cartesian configuration (neurosurgery 3D orientation surgical robot which was developed by Switzerland Swiss Federal Research Institute). We used cylindrical configuration, because of its advantages compared to others, such as smaller and larger workspace, higher precision positioning and human-robot interaction. Fig. 3 shows the workspace of MWA treatment for liver cancer using an ultrasound imaging system.



Fig. 3 Workspace of MWA treatment for liver cancer

Considering the medical environment, the robot should have sufficient strength, accuracy, safety and dexterity. Based on the above operation requirements, we designed the articulated manipulator robot as shown in Fig. 4.

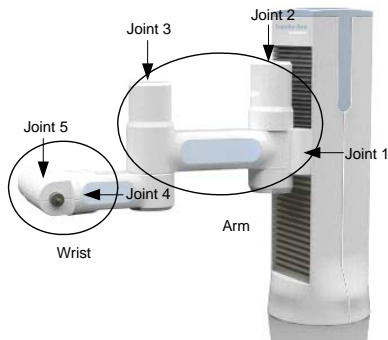


Fig. 4 Medical robot arm and wrist structure

4.2 Robot wrist

The orientation of the surgical tools is controlled by the robot wrist. Fig. 5 shows the detailed antenna in ablation. Qinjun DU, a member of our research group, has discussed the detailed wrist design (Du et al., 2006). Based on the requirement of MWA treatment, we designed the wrist with a 2-DOF structure (Fig. 4).

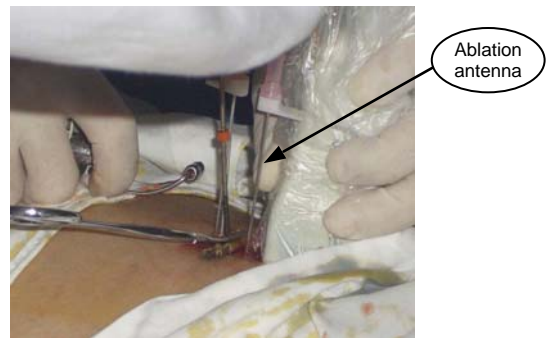


Fig. 5 Ablation antenna position and orientation

Finally, we integrated the robot's mechanic, control unit, cabling and outward appearance design. The prototype of our robot is shown in Fig. 6.



Fig. 6 CAD model (a) and prototype of the robot (b)

The safe issue is an important aspect on medical robot (Fei and Ng, 2001). We considered three aspects of safety. Firstly, the robot system is used only to

assist positioning, and the final insertion is operated by the surgeon, guided by ultrasound images. Secondly, every motor is equipped with a brake on the back, and after the robot has the correct position, the brake will lock the motor axis and the motor power will be cut off. Thirdly, the trajectory planning of the manipulator is placed over the lesion during the surgical operation, and the manipulator itself cannot directly contact the patient.

5 Kinematic analysis

Kinematic analysis in this system is mainly on two coordinates: robot coordinate and EM tracking system coordinate (EM coordinate). Robot coordinate is used for the robot's manipulation during the treatment; EM coordinate is used in two areas: monitoring the robot wrist and reconstructing the tissue with 2DUS images.

The 5-DOF needle placement robot is a low-DOF robot; the wrist designed here has a more compact mechanical structure, however, the robot structure cannot be easily obtained through algebraic solutions. Thus, we proposed a combined numerical method, and main kinematic analysis is given as below.

5.1 Forward kinematic analysis

To decide the position and orientation of the end-effector of manipulators, it is necessary to establish a kinematic equation relating the joint space to the coordinate space. The coordinate frame of adjacent links is shown in Fig. 7.

We calculated the direct kinematic equation according to the D-H method. The kinematics equation is

$${}^rT_5 = \begin{bmatrix} C_4C_5C_{23} + S_5S_{23} & -S_4C_{23} & -C_4S_5C_{23} + C_5S_{23} & d_4S_{23} + a_2C_2 \\ C_4C_5S_{23} - S_5C_{23} & -S_4S_{23} & -C_4S_5S_{23} - C_5C_{23} & -d_4C_{23} + a_2S_2 \\ S_4C_5 & C_4 & -S_4S_5 & d_1 \\ 0 & 0 & 0 & 1 \end{bmatrix} \quad (1)$$

where

$$C_4 = \cos \theta_4, C_5 = \cos \theta_5, C_{23} = \cos (\theta_2 + \theta_3), \\ S_2 = \sin \theta_2, S_4 = \sin \theta_4, S_5 = \sin \theta_5, S_{23} = \sin (\theta_2 + \theta_3).$$

5.2 Inverse kinematic analysis

For low-DOF robots, we can only obtain two values of columns in target's matrix. As the robot's wrist has a more compact mechanical structure, the robot structure cannot be easily described by algebraic solutions. Thus, we have proposed a combined numerical method for this robot structure. The detailed process is as follows.

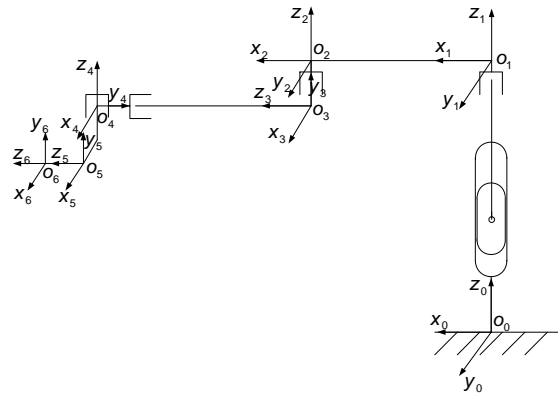


Fig. 7 Coordinate frame of adjacent links

Step 1: we order one joint angle as a known value, which increases incrementally from the minimum to the maximum of the joint angle range.

Step 2: based on the known joint angle, we can compute the inverse kinematic solution with an algebraic method. Simultaneously, we examine the domain of the trigonometric functions of the joint angles.

Step 3: if Step 2 returns all five joint angles without exceeding the requirements, the computed result is the robot's numerical solution; if not, the computed process should return to Step 1 to iteratively derive the solution. If the known value arrives at the maximum of joint angle range, then the process proceeds to Step 4.

Step 4: we analyze the iterative results and obtain the solution.

5.3 Coordinate mapping between robot and EM

The target position and orientation in the EM device coordinate is ${}^{em}T_r$, the EM device coordinate in robot base coordinate is ${}^rT_{em}$, so the target position and orientation in robot base ${}^rT_r = {}^rT_{em} {}^{em}T_r$ (Fig. 8).

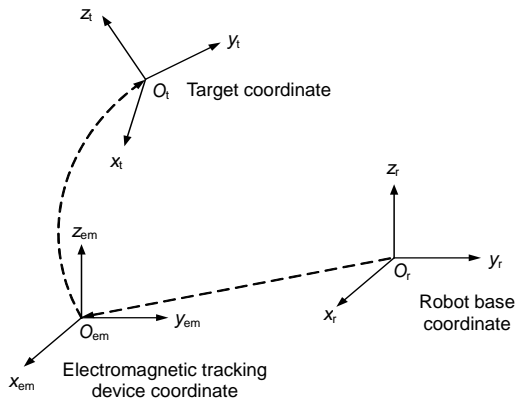


Fig. 8 Coordinate mapping

6 Experiment

The experiment was performed to test the accuracy of the robot. The experiment flow is as follows. First, we marked a point (Fig. 9) beside the arm’s guiding hole; then randomly selected a preset point within the robot’s workspace and solved the joint angles with inverse kinematics. We then manipulated the robot arm to the preset point and measured the real position of the marked point with a coordinate measure machine after manipulation. Finally, we defined that q_{preset} and q_{arrived} are the 3D positions of the preset point and arrived point, respectively. Then we calculated the error in Euclidian space with Eq. (2):

$$\text{err} = \|q_{\text{preset}} - q_{\text{arrived}}\|. \tag{2}$$



Fig. 9 Accuracy test of the needle guiding robot

This experiment was repeated 5 times with 5 different preset points as shown in Tables 3–5.

The error mainly comes from the harmonic backlash, and the servo’s error also has a small con-

tribution to the robot’s error. From the data above, it is seen that the 5-DOF needle-placement robot’s accuracy is less than 0.5 mm, which meets the requirements of a robot for MWA in liver cancer treatment.

Table 3 The preset and actually arrived points along axis X (mm)

Test point No.	Preset	Measured	Error
1	533.2	533.0	0.2
2	499.3	499.2	0.1
3	466.6	466.8	0.2
4	410.3	410.5	0.2
5	366.6	366.7	0.1

Table 4 The preset and actually arrived points along axis Y (mm)

Test point No.	Preset	Measured	Error
1	61.3	61.5	0.2
2	43.7	43.8	0.1
3	31.7	31.5	0.2
4	16.6	16.5	0.1
5	-36.2	-36.4	0.2

Table 5 The preset and actually arrived points along axis Z (mm)

Test point No.	Preset	Measured	Error
1	80.7	80.9	0.2
2	60.8	70.0	0.2
3	70.6	70.4	0.2
4	10.2	10.1	0.1
5	30.2	30.3	0.1

In addition, we also have conducted animal trials (Fig. 10). Experiment results show that the robot mechanical design also meets the requirements of MWA treatment. In the animal experiments, the respiration motion mostly influences the robotic system’s accuracy, however, this topic will be dealt with in future studies.



Fig. 10 Experiment on animals (pig). (a) Ultrasound scanning; (b) Robot assisting needle placement

7 Conclusion

According to the requirements of MWA treatment in liver cancer, we have designed a compact ultrasound-directed robot for needle-positioning.

The system allows for detailed kinematic analysis, including a combined numerical algorithm to compute the robot's inverse kinematic solutions, path planning and coordinate mapping between different coordinates. Finally, experimental results show that the robot's accuracy meets the operation requirements for MWA in liver cancer. To date now, we have conducted several animal trials. After further animal trials, clinical trials will be considered.

References

- Boctor, E.M., Fischer, G., Choti, M.A., Fichtinger, G., Taylor, R.H., 2004. A Dual-armed Robotic System for Intraoperative Ultrasound Guided Hepatic Ablative Therapy: A Prospective Study. *Proceedings of IEEE ICRA*, New Orleans, p.2517-2522.
- Cleary, K., Nguyen, C., 2001. State of the art in surgical robotics: Clinical applications and technology challenges. *Computer Aided Surgery*, **6**(6):312-328. [doi:10.3109/10929080109146301]
- Colombo, M., 1992. Hepatocellular carcinoma. *Hepatology*, **15**(4):225-236. [doi:10.1002/hep.1840150421]
- Du, Q.J., Huang, Q., Tian, L.B., Liu, C.C., 2006. Mechanical Design and Control System of a Minimally Invasive Surgical Robot System. *Proceeding of IEEE ICMA*, Luoyang, China, p.1120-1125.
- Du, Q.J., Zhang, X.Y., 2006. Manipulability Analysis and Design of Radio Frequency Ablation Robot. *Proceeding of IEEE WCICA*, Chongqing, China, p.7432-7437.
- Esquivel, C., Keeffe, E., Garcia, G., Imperial, J., Millan, M., Monge, H., So, S., 1999. Hepatic neoplasm: Advances in treatment. *Gastroenterol Hepatol*, **14**(suppl):37-41.
- Fei, B.W., Ng, W.S., 2001. The safety issues of medical robotics. *Reliability Engineering and System Safety*, **73**(2):183-192. [doi:10.1016/S0951-8320(01)00037-0]
- Seki, T., Wakabayashi, M., Nakagawa, T., Itoh, T., Shiro, T., Kunieda, K., Sato, M., Uchiyama, S., Inoue, K., 1994. Ultrasonically guided percutaneous microwave coagulation therapy for small hepatocellular carcinoma. *Cancer*, **74**(3):817-825. [doi:10.1002/1097-0142(19940801)74:3<817::AID-CNCR2820740306>3.0.CO;2-8]
- Seki, T., Wakabayashi, M., Nakagawa, T., Imamura, M., Tamai, T., Nishimura, A., Yamashiki, N., Okamura, A., Inoue, K., 1999. Percutaneous microwave coagulation therapy for patients with small hepatocellular carcinoma. *Cancer*, **85**(8):1694-1702. [doi:10.1002/(SICI)1097-0142(19990415)85:8<1694::AID-CNCR8>3.0.CO;2-3]
- Tsai, Y.C., Soni, A.H., 1984. The effect of link parameter in the working space of general 3R robot arms. *Mechanism and Machine Theory*, **19**(1):9-16. [doi:10.1016/0094-114X(84)90004-1]
- Tsai, Y.C., Soni, A.H., 1985. Workspace synthesis of 3R, 4R, 5R and 6R robots. *Mechanism and Machine Theory*, **20**(6):555-563. [doi:10.1016/0094-114X(85)90072-2]
- Ye, S.L., Qin, S.K., 2009. Expert consensus of standardized treatment of primary liver cancer. *Tumour*, **4**:295-304.
- Ying, X., Ma, X.F., 1991. Synthesis of types of manipulators and determination of their structural parameters in mechanical system design of robots. *Journal of University of Science and Technology Beijing*, **13**(3):252-258.